SRC TR 85-53

Geophysical Inversion and Two-Dimensional Signal Processing

by

P. S. Krishnaprasad

and

G. Blankenship

Report Documentation Page

Form Approved
OMB No. 0704-0188

1. REPORT DATE	2. REPORT TYPE	3. DATES COVERED
20 APR 1985		**00-00-1985 to 00-00-1985**

4. TITLE AND SUBTITLE	5a. CONTRACT NUMBER
Geophysical Inversion and Two-Dimensional Signal Processing	5b. GRANT NUMBER
	5c. PROGRAM ELEMENT NUMBER
6. AUTHOR(S)	5d. PROJECT NUMBER
	5e. TASK NUMBER
	5f. WORK UNIT NUMBER
7. PERFORMING ORGANIZATION NAME(S) AND ADDRESS(ES) **University of Maryland,Electrical Engineering Department,College Park,MD,20742**	8. PERFORMING ORGANIZATION REPORT NUMBER
9. SPONSORING/MONITORING AGENCY NAME(S) AND ADDRESS(ES)	10. SPONSOR/MONITOR'S ACRONYM(S)
	11. SPONSOR/MONITOR'S REPORT NUMBER(S)

12. DISTRIBUTION/AVAILABILITY STATEMENT
Approved for public release; distribution unlimited

13. SUPPLEMENTARY NOTES

14. ABSTRACT
see report

15. SUBJECT TERMS

16. SECURITY CLASSIFICATION OF:			17. LIMITATION OF ABSTRACT	18. NUMBER OF PAGES	19a. NAME OF RESPONSIBLE PERSON
a. REPORT	b. ABSTRACT	c. THIS PAGE			
unclassified	**unclassified**	**unclassified**		**44**	

Geophysical Inversion

and

Two-Dimensional Signal Processing

Final Report

of

Contract: N00014-84K-2008

Prepared by:

P.S. Krishnaprasad and G. Blankenship

Department of Electrical Engineering

University of Maryland

College Park, Maryland 20742

Date: August 20, 1985

Geophysical Inversion

and

Two-Dimensional Signal Processing

Abstract: This report is motivated by the need to understand the possible applications of two-dimensional (2-D) modeling of stochastic processes and related techniques in signal processing to problems of inversion of geophysical data. Here we first provide a brief overview of 2-D modeling and signal processing techniques. We then address the problem of passing from free air gravity anomaly data (FAG) to bathymetry. We present an approach to this fundamental inversion problem, based on a systematic spatial segmentation of the 2-D data followed by statistical modeling within the segments. We also suggest possible improvements on current approaches based on transfer function methods.

Geophysical Inversion

and

Two-Dimensional Signal Processing

Table of Contents

1. Introduction:

It is now possible to obtain very reliable mappings of the earth's gravity field using air-borne gravimeters. Measurements of sea-level using radar or laser altimeters on satellites also provide a wealth of information concerning the geoid. Typically the data is collected along tracks followed by the instrument-bearing platform. The tracks provide a grid like pattern of data to be used for inversion purposes, e.g. inverting FAG to bathymetry. Current practice in this field is based on modeling and signal processing methods that are intrinsically one dimensional (along the data-collection tracks) in nature. To make effective use of such techniques, it is also customary to assume certain directional uniformity properties perpendicular to the tracks. From the point of view geophysics, such assumptions may be unnatural. Also, processing along tracks often implies only partial use of the information at hand. These and other reasons, motivated us to investigate the possibility of using the methods of two dimensional stochastic modeling for the purposes geophysical inversion.

In the present report, we begin by giving a brief overview of certain aspects of the theory of 2-D random fields in section 2. We focus primarily on certain recent developments in 2-D autoregressive moving average (ARMA) type models. An important idea in our work is that when such models are constructed for FAG data, they will be valid only over limited regions of the earth, in part determined by the 'largest wavelength' appropriate for the data. It is therefore necessary to properly *segment* the FAG data into various spatial regions and construct models within the regions. Our approach to segmentation is based on detecting

edges across which large changes in FAG data arise. We discuss a class of techniques for detecting edges in FAG data in section 4. (The methods may be of independent geophysical interest than for inversion.)

In section 4.1, we present our approach to the use of two dimensional modeling techniques for the problem of inverting from FAG data to bathymetry. We give details of our estimation technique and segmentation technique in sections 4.2 and 4.3. In section 4.4, we present a brief discussion of some recent advances in the theory of deconvolution. We think that these new results could be of considerable use in modeling and inversion based on transfer functions.

The final section 5 contains proposals for future work. Among other things, we believe that detailed studies of sea bottom roughness models may help make our statistical techniques more reliable.

2. Parametric Models for 2-D Random Fields:

A basic problem associated to an array of (random) data on a two-dimensional "grid" is that of reconstructing the underlying signal corresponding to the data. Based on their success in treating one dimensional signals, parametric models are highly desirable in this instance also. Two dimensional analogues of ARMA models can be introduced for this purpose. We do so following a preliminary discussion of random fields.

2.1. Random Fields

A stochastic process over T is a family of random variables indexed by a parameter set T. We denote this family as $\chi \triangleq \{X_t : t \in T\}$. Here we assume that the random variables X_t take vallues in a vector space - typically $\mathbb{C}^N$. If N $= 1$, it is customary to refer to χ as a univariate stochastic process.

Usually, the index set T denotes time, i.e. $T = \mathbb{R}$ or Z. However if T is a multidimensional space, we say that χ is a *random field.* For our purposes, we will mostly restrict attention to $T = \mathbb{R}^2$ (random field on a plane) or $T = Z^2$ (random field on a planar grid or lattice).

Many important concepts from the theory of stochastic processes over $\mathbb{R}$ (or Z) generalize to random variables over $\mathbb{R}^n$ (or Z^n).

We say that a univariate random field χ over $\mathbb{R}^n$ (or Z^n) taking values in $\mathbb{C}$ is *homogeneous* if,

$$E(X_t) = \mu \quad \forall t \in \mathbb{R}^n \ (or\ Z^n),$$

and

$$E(X_{t+\tau}\overline{X}_{t'+\tau}) = E(X_t\,\overline{X}_{t'}), \quad \forall t, t', \tau \in \mathbb{R}^n \text{ (or } Z^n).$$

We denote as $R(t-t')$ the *correlation* $E\{(X_t - E(X_t))\overline{(X_{t'} - E(X_{t'}))}\}$ of a given homogeneous random field. It is important to note that $R(t-t')$ is *non-negative definite,* i.e., given a set $\{a_1, \ldots, a_m\}$ of complex numbers, m an arbitrary positive integer,

$$\sum_{i=1}^{m}\sum_{j=1}^{m} a_i\,\overline{a}_j\,R(t_i - t_j) \geq 0$$

for any choice $\{t_1,\ldots,t_m\} \subseteq \mathbb{R}^n$ (or Z^n).

It follows by a famous theorem of Bochner and Herglotz that we have a (spectral) representation,

$$R(t) = \int_{\substack{\mathbb{R}^n \\ \text{or} \\ T^n}} e^{i<\nu,t>}\, dF(\nu). \tag{2.1.1}$$

(Here T^n denotes the n-torus). F is a measure known as the *spectral measure.* When it is possible to write,

$$dF(\nu) = S(\nu)\,d\nu,$$

we say that $S(\nu)$ is the *spectral density* of the given random field.

Homogeneous random fields are singled out for modeling data sets that appear to possess a translation invariance property in their correlation. A further special class of random fields of importance is the class of *homogeneous and isotropic* random fields satisfying;

$$E(X_t) = \mu = 0 \quad \forall t \in \mathbb{R}^n \text{ (or } Z^n),$$

and

$$E(X_t, \overline{X}_{t'}) = E(X_{P(t)}\overline{X}_{P(t')}) \quad \forall t, t' \in \mathbb{R}^n \text{ (or } Z^n),$$

and the map $t \to P(t)$ denotes a rigid motion in $\mathbb{R}^n$ (or Z^n). Recall that a rigid

motion in $\mathbb{R}^n$ is a combination of rotation and translation. Thus, for a planar, homogeneous and isotropic random field to be a good model for a given data set, the latter should have both translational and rotational invariance properties in its statistics.

It follows that

$$E(X_t \overline{X}_{t'}) = R(||t - t'||) \tag{2.1.2}$$

is a function only of the Euclidean distance $||t - t'||$ (or the lattice distance). A very nice theorem analogous to Bochner-Herglotz holds.

Theorem:

A function $R(\nu)$, $0 \leq \nu < \infty$ is the correlation function of an isotropic and homogeneous random field over $\mathbb{R}^n$ iff,

$$R(r) = \int_0^\infty \frac{J_{(n-2)/2}(\lambda r)}{(\lambda r)^{(n-2)/2}} dF_0(\lambda). \tag{2.1.3}$$

(For n=2, $R(r) = \int_0^\infty J_0(\lambda r)\, dF_0(\lambda)$)

Here J_0= Bessel function of order 0, etc.

Remark 2.1.1: This theorem tells us how to pass correctly from correlation functions to spectral density functions. The ordinary Fourier transform is *not* the right thing to use for homogeneous and isotropic random fields.

Remark 2.1.2: For data in 2 dimensions, a plot of the correlation function should reveal radial symmetry if present and suggest what class of random field models to use. We will in any case always make the assumption that *homogeneity* is valid for FAG data *if the data is restricted to a reasonably sized segment.* Precisely how to determine the segmentation will be one of our major concerns.

Before we close this section, we note that the property of Markovianness which plays a key role in connection with stochastic processes over $\mathbb{R}$ has a considerably more complex theory in the case random fields. One definition based on conditional independence has the associated picture:

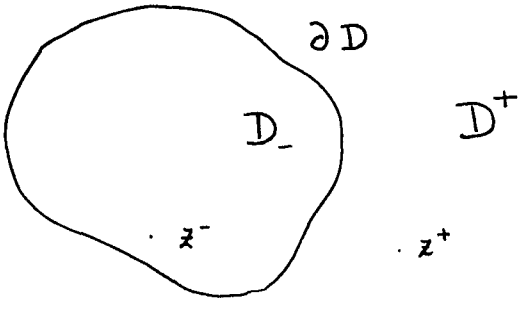

$\{X_z : z \in \mathbb{R}^2\}$ is Markov if for any region D – as above, X_{z-} and X_{z+} are independent, conditioned on $\{X_z : z \in \partial D\}$. We shall see below in section (2.3) that a different notion of Markovianness is needed.

Since we are primarily concerned with gridded FAG data, we shall confine all our discussions on modeling to 2-D random fields over the planar lattice.

2.2. Models for 2-D Discrete Random Fields:

From 2-D linear system theory, we have the notion of an input-output system as a discrete convolution;

$$Y(n_1,n_2) = (I-H * X)(n_1,n_2)$$

$$= \sum_{m_1=-\infty}^{\infty} \sum_{m_2=-\infty}^{\infty} h(n_1 - m_1, n_2 - m_2)X(m_1, m_2) \qquad (2.2.1)$$

where $X(\cdot,\cdot)$ is an *input* and $Y(\cdot,\cdot)$ is the corresponding *output* and $h(\cdot,\cdot)$ denotes the *impulse response* or *weighting pattern*.

The system (2.2.1) is causal if,

$$h(n_1,n_2) = 0 \quad \forall n_1,\ n_2<0. \tag{2.2.2}$$

The weighting pattern $h(\cdot,\cdot)$ is said to be separable if

$$h(n_1,n_2) = f(n_1)g(n_2) \quad \forall n_1,n_2\in Z. \tag{2.2.3}$$

Much of 2-D realization theory, [Bose 1982, Multidimensional System Theory] is concerned with conditions on weighting patterns satisfying (2.2.2) that can be realized as, *difference equations* of the form,

$$\sum_{m_1=0}^{M_1}\sum_{m_2=0}^{M_2} \alpha_{m_1,m_2}\, Y(n_1-m_1,\ n_2-m_2) \tag{2.2.4}$$

$$= \sum_{l_1=0}^{L_1}\sum_{l_2=0}^{L_2} \beta_{l_1,l_2}\, X(n_1-l_1,\ n_2-l_2).$$

If $Y(\cdot,\cdot)$ and $X(\cdot,\cdot)$ are random fields and if we let $X(\cdot,\cdot)$ be a discrete 2-D white noise process, then (2.2.4) becomes the analogue of the notion of ARMA model widely used in time series analysis [Box Jenkins 1971 Time Series].

We say that H is stable if in (2.2.1) we get bounded outputs for bounded inputs. We note,

Theorem (Stability):

Let $H(z_1,z_2) = \sum_{n_1=-\infty}^{\infty}\sum_{n_2=-\infty}^{\infty} h(n_1,n_2)z_1^{-n_1}z_2^{-n_2}$ and assume that H is casual and of the form, $H(z_1,z_2) = \dfrac{A(z_1,z_2)}{B(z_1,z_2)}$. Then H is stable if it is analytic in $|Z_1|\geq 1,\ |Z_2|\geq 1$.

While the subject of causal 2-D models is of independent interest there is *no compelling reason* for us to work with such models in the present context of geophysical fields. One would however expect geophysical data to satisfy certain

relations between field values associated to points in a given lattice neighborhood of a lattice point. Thus, we are in a situation where *noncausal* 2-D models generalizing (2.2.4) are needed. One class of such models is given by the following:

$$X_{r,s} = \sum_{i=1}^{n} a_i (X_{r-i,s} + X_{r+i,s}) +$$

$$+ \sum_{j=1}^{n} b_j (X_{r,s-j} + X_{r,s+j}) + W_{r,s} \qquad (2.2.5)$$

Here $\{W_{r,s};\ -\infty<r<\infty\ ,-\infty<s<\infty\}$ is the 2-D analog of discrete time white noise, satisfying

$$E(W_{r,s}) = 0$$

$$cov(W_{r,s}, W_{r',s'}) = \delta(r-r',\ s-s')\, q, \qquad q>0$$

($\delta(i,j)$ is the usual Kronecker symbol). Models of this type are investigated in the elegant volume [Bartlett 1976, Spatial Patterns]. In the special case,

$$X_{r+1,s+1} = a_1 X_{r,s+1} + a_2 X_{r+1,s} \qquad (2.2.6)$$

$$- a_1 a_2 X_{r,s} + W_{r,s}$$

we get an *exponential* correlation of the form,

$$R_{XX}(i,j) \triangleq E(X_{r,s} X_{r+i,s+i})$$

$$= \sigma^2 \exp[-c_1 |i| - c_2 |j|] \qquad c_1, c_2>0. \qquad (2.2.7)$$

The parameter c_1, c_2 and σ^2 in the correlation function are related to the parameters of the casual model (2.2.6) by the following formulas:

$$a_1 = \exp(-c_1)$$

$$a_2 = \exp(-c_2) \qquad (2.2.8)$$

$$q = \sigma^2 (1 - a_1^2)(1 - a_2^2).$$

From (2.2.8), it is clear that one can estimate the parameters of the model (2.2.6), if indeed the data justifies a correlation function of the form (2.2.7).

Non-causal models of the form (2.2.5), (2.2.6) and their variants are of interest to us as candidates for geophysical problems. There are two fields of interest to us: (a) the free air gravity (FAG) field and (b) the bathymetry field. In what follows, we shall be concerned with imposing the proper constraints on noncausal models in order to be useful for the solution of geophysical problems.

2.3. Periodic Random Fields:

The random fields of section (2.2) were assumed to be defined over the *entire* planar lattice. This conflicts with two important factors:

- for a geophysical field such as FAG data or bathymetry, one *cannot* reasonably expect spatial homgeneity properties outside a certain window or segment; *different* parts of the world should obey different local regularities (models).
- practical limitations of data collection confine one to such a window to begin with.

Thus we are forced to impose additional window constraints. It is quite obvious that these considerations are not unique to 2-D models. In fact the above remarks apply equally well to 1-D models. In his book on time series, Hannan [Hannan 1960, Time Series] considered a class of processes that are periodic, i.e. satsify a constraint of the form,

$$Y_{k+Nm} = Y_k \quad \forall k, m \in Z \tag{2.3.1}$$

(N = window size)

In the present context, one can apply the same idea to a noncausal random field

model, namely to define the field simply by *periodic extension* outside a window of size $N_1 \times N_2$. As we shall see below, this has important consequences for computations as well. In several recent papers, Kashyap and Chellappa have analyzed an important special class of noncausal 2-D periodic random field models [Kashyap 1981, Image Modeling][Chellappa, Kashyap 1979 Decision Rules] [Chellappa 1980 Spatial Autoregressions]. For a variety of reasons that will be apparent in section 4, we adopt precisely this class of models as candidate models for geophysical fields.

Let a 2-D discrete real random field $\{Y_{i,j} : i,j \in Z\}$ be given by an autoregressive model of the form,

$$Y_{i,j} + \sum_{k=1}^{m} \theta_k Y_{i+q_k^1, j+q_k^2} = \beta^{\frac{1}{2}} U_{i,j} \tag{2.3.1}$$

here $Q := \{(q_k^1, q_k^2): k = 1,2,\ldots,m\}$ is a subset of $Z \times Z$ identifying the appropriate neighborhood of lattice points associated to a given one. The θ_i are scalar weights, $U_{i,j}$ is a discrete 2-D random field corresponding to Gaussian white noise; $E[U_{ij}] = 0$ and $Var[U_{i,j}] = 1$.

The model (2.3.1) is taken together with a periodicity condition,

$$Y_{i+kN_1, j+lN_2} = Y_{i,j} \quad \forall i,j,k,l \in Z. \tag{2.3.2}$$

Here N_1 and N_2 are positive integers determining the window or segment of homogeneous behavior. We shall be concerned with modeling using only data from within the window

$$W := \{(i,j): 1 \leq i \leq N_1; 1 \leq j \leq N_2\}. \tag{2.3.3}$$

A typical example of Q might be

$$Q := \{(-1,0), (0,-1), (1,0), (0,1), (1,1)\}. \tag{2.3.4}$$

The corresponding neighborhood can represented as in Fig. 2.3.1.

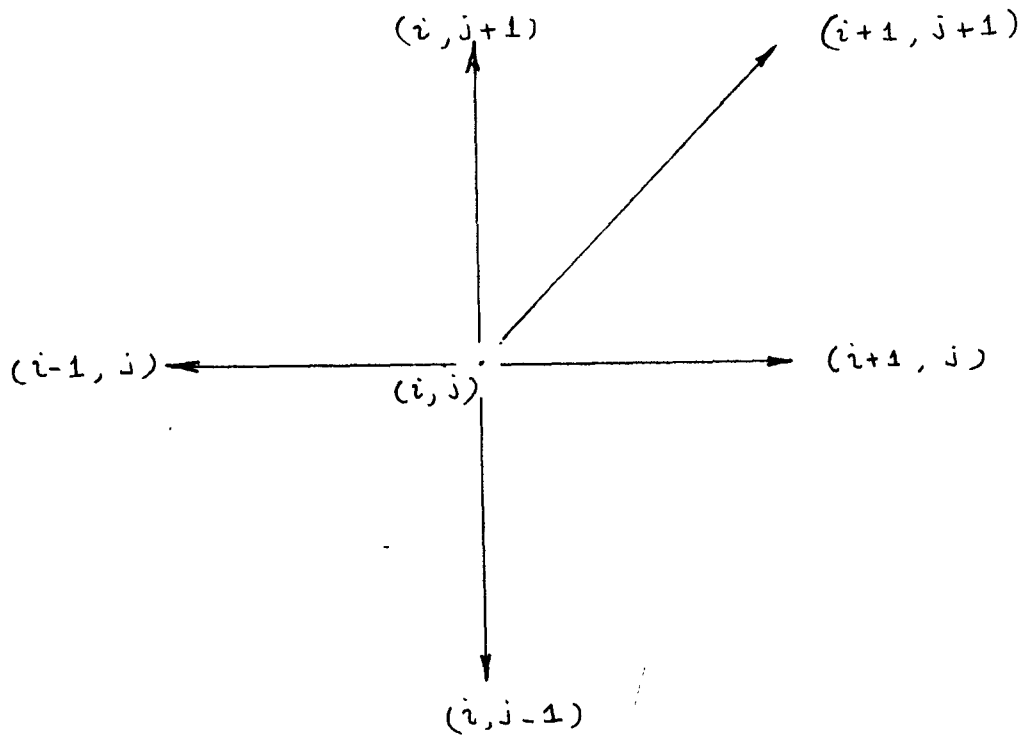

Figure 2.3.1

In section 4 below we analyze the class of models (2.3.1) - (2.3.2) and give formulas for estimation of parameters. It should be borne in mind that the parameters of the model consist of the tuple $(Q, \theta, N_1, N_2, \beta)$ where $\theta = (\theta_1,\ldots,\theta_m)^T$.

In general the models (2.3.1) - (2.3.2) *do not* satisfy the usual Markov property, i.e. Prob density $\{Y_{i,j} \mid Y_{l,p}; (l,p) \neq (i,j)\}$

$$\neq \text{Prob density } \{Y_{i,j} \mid Y_{l,p}; \tag{2.3.5}$$

$$l = i + q_k^1$$

$$p = j + q_k^2$$

$$(q_k^1, q_k^2) \in Q \}$$

However (2.3.5) is indeed an equality if Q in (2.3.5) is replaced by some $Q_1 \supset Q$.

3. Current Practice in Geophysical Inversion:

The main problem of gravity interpretation is that of inferring a plausible subsurface density distribution (or subsurface body) from surface observations of the free air gravity anomaly (FAG). More specifically, based on (FAG) data over the ocean, we seek to infer the bathymetry. There are a variety of sources of nonuniqueness in the inversion process. One example is that of density distributions of rapidly oscillating positive and negative densities at depth. Also more seriously, geophysical processes such as *isostatic compensation* lead to nonuniqueness. We make some remarks about current practice in this area.

3.1. Discrete Inverse Theory:

At present, two basic approaches are used:

(a) model the gravity anomaly by means of of one or more constant-density bodies with *variable geometry,* such as a sphere, cylinder, prism, polygon, a set of prisms to model an interface etc. The geometry of the disturbing body is iteratively adjusted from a starting point;

(b) *fix the geometry* of the model (for example a regular array of identical rectangular or square blocks) and allow the densities of the blocks to vary.

In connection with approach (a), both spatial and frequency domain methods

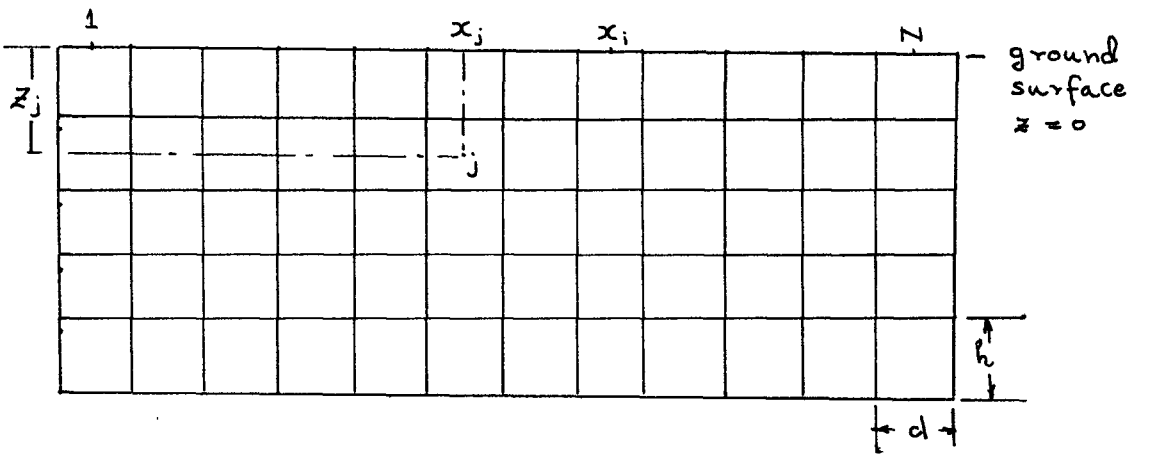

Figure 3.1 (Last a Kubik 1983)

d and h are the horizontal and vertical dimensions of an elementry block. Density of j th block is ν_j.

have been used [Oldenburg 1974 gravity anomalies], [Bhattacharya Leu 1975 gravity and magnetic anomalies], [Pedersen 1978 statistical potential fields], [Pedersen 1979 Wavenumber domain].

In connection with approach (b) there are substantial difficulties in reducing the nonuniqueness. However, recent efforts in this direction include the use of quadratic programming and monotonicity assumptions on the density [Fisher Howard 1980 Gravity interpretation quadratic programming] and "compactification," or minimizing the volume of the causative body [Last Kubik 1983 Compact gravity]. We recall here the basic model of [Last Kubik 1983 Compact gravity].

Consider Figure 3.1. The data is collected along a track. The geometry is fixed, but the density is allowed to vary from block to block. The model for gravity at ith data point is

$$g_i = \sum_{j=1}^{M} a_{ij}\nu_j + e_i \quad i = 1,2,\ldots,N \tag{3.1.1}$$

where ν_i = density of jth block, e_i = noise associated to ith measurement and, a_{ij} = matrix element representing the influence if the jth block on the ith gravity value. From standard arguments [Garland 1965 Earth's Shape and Gravity] we know,

$$\begin{aligned} a_{ij} = 2\gamma[(x_i - x_j + d/2)\log(\frac{r_2 r_3}{r_1 r_4}) \\ + d\log(\frac{r_4}{r_3}) \\ - (z_j + h/2)(\theta_4 - \theta_2) \end{aligned} \tag{3.1.2}$$

$$+ (z_i - h/2)(\theta_3 - \theta_1)]$$

where,

$$\begin{aligned}
r_1^2 &= (z_j - h/2)^2 + (x_i - x_j + d/2)^2, \\
r_2^2 &= (z_j + h/2)^2 + (x_i - x_j + d/2)^2, \\
r_3^2 &= (z_j - h/2)^2 + (x_i - x_j - d/2)^2, \\
r_4^2 &= (z_j + h/2)^2 + (x_i - x_j - d/2)^2, \\
\theta_1 &= \tan^{-1}(x_i - x_j + d/2)/(z_j - h/2), \\
\theta_2 &= \tan^{-1}(x_i - x_j + d/2)/(z_j + h/2), \\
\theta_3 &= \tan^{-1}(x_i - x_j - d/2)/(z_j - h/2), \\
\theta_4 &= \tan^{-1}(x_i - x_j - d/2)(z_j + h/2).
\end{aligned} \tag{3.1.3}$$

Here γ is the universal gravitational constant.

It follows that one can set up the problem as that of solving for a vector V of densities satisyfing,

$$G = AV + E, \tag{3.1.4}$$

where G is the vector of gravity data. One typically solves (3.1.4) using least squares. There are various approaches to *regularizing* the problem including the compactification idea of Last and Kubik. It is customary to use weighted least squares.

More recently certain implementations of one dimensional track inversion have become available that are iterative but not based on least squares. We discuss one below.

3.2. The Algorithm of Lipman:

This particular algorithm has been implemented and tested and is discussed in a report [Rosenblum 1983 gravity to bathymetry inversion]. Since the details are available in the report, we limit ourselves to highlighting the main features of the algorithm:

(a) the method is iterative starting from an initial mean bathymetry such that the corresponding FAG $\equiv 0$;

(b) it adjusts the bathymetry by adding or subtracting mass (via prisms) at each point;

(c) it assumes uniform density along a track;

(d) the iteration G based on attempting to bring the *computed* FAG at each point to some value not further than a tolerance ϵ (in mgals) from the corresponding FAG;

(e) it includes a constraint on slope to avoid spiking;

(f) the realization of step (d) above is based on two elements - a decision rule that determines whether a region which violates the predefined tolerance ϵ in (d) above is 'fixable' - i.e. improved to within tolerance without adversely affecting points outside this region but 'nearby'.

(g) once a region has been found to be fixable, new prismatic masses are added using a routine called SLABADD.

The above algorithm does not explicitly use a goodness-of-fit measure as in least squares. In its current implementation, the algorithm requires the following user-defined input parameters:

(a) the FAG data point spacing in the data file (in km);

(b) the average depth along the track (in km);

(c) the average density (assumed constant);

(d) the maximum error allowed in fitting the estimated FAG to the measured FAG (in mgals, usually 2-4 mgals);

(e) the bathymetric stepsize allowed (in kms, about 1/5 the data point spacing in (a) above);

A certain amount of user-sophistication appears to be necessary in order to ensure adequate performance of the algorithm. In the next sub-section, we make some comments on current practice in order to set the context for our proposed approach.

3.3. Some Comments on Current Inversion Techniques:

To the best of our knowledge, all currently used techniques are based on processing data along tracks, i.e. these are 1-D methods. This implies that for the least squares methods of section 3.1., one has to use uniform prisms that are of infinite extent perpendicular to the tracks. In the regions of the earth where such directional homogeneity is unavailable, the use of 1-D methods is at best a rough and ready approximation. However, direct extensions of the methods of section (3.1) to 2-D data lead to considerable computational problems. Formulas analogous to (3.1.2) and (3.1.3) can be written down, but are difficult to analyze for the purposes of determining whether or not "influence matrices" such as A in (3.1.4) are approximated by sparse matrices. Such considerations are essential in

order to make the problem computationally tractable.

We propose that a different approach based on discrete 2-D random field models be considered for the purposes of inversion. The details are given in the next section. The main point of our approach is that we propose model building based on sound statistical principles. The class of models that we consider is that of periodic random fields introduced in (2.3).

4. Geophysical Modeling and Inversion Using 2-D Discrete Random Fields:

In this section, we present our *algorithm* for modeling and inversion of 2-D random fields associated to the problem of inversion from FAG to bathymetry. The basic random fields for us are the univariate fields of free air gravity and bathymetry, denoted as G_{ij} and B_{ij} respectively. For computational reasons, we restrict ourselves to univariate techniques. The basic steps are given in section 4.1. The details of the estimation procedure (following Kashyap) are given in 4.2. The procedure in (4.1) assumes that a prior segmentation of the field in question has been given. In order to obtain such a segmentation or windowing we discuss in section (4.3) a method that has its origins in image processing. This is a deterministic two-stage technique involving first a convolution with the gravity field by a suitable kernel followed by nonlinear processing. In comparison with a statistical technique proposed by Kashyap, this method appears to be much less computation-intensive and has performed well in experiments on real images. Our idea is to apply this technique to the gravity anomaly data and segment it before doing any detailed modeling.

The last section of this chapter is denoted to some recent advances in deconvolution techniques. We believe that these new tools could be of great utility in inversion algorithms based on transfer function models.

4.1. The Modeling and Inversion Algorithm:

We use the notation of section (2.3). Recall, from that section that a periodic random field model obeys a law of the form:

$$Y_{ij} + \sum_{k=1}^{m} \theta_k Y_{i+q_k^1, j+q_k^2} = \beta^{\frac{1}{2}} U_{ij} \quad 1 \leq i \leq N_1,\ 1 \leq j \leq N_2,$$

$$Y_{i+kN_1, j+lN_2} = Y_{ij} \quad \forall i, j, k, l \in Z. \tag{4.1.1}$$

Here N_1 and N_2 determine the window size and $Q = \{(q_k^1, q_k^2)\ k = 1,2,\ldots,m\} \subset Z \times Z$ determines neighborhood dependence. The field $\{U_{ij}\}$ is a standard discrete Gaussian white noise field. We find it convenient to adapt the well-known polynomial model notation as follows:

Let s_1 and s_2 denote the following shift operators,

$$s_1 Y_{i,j} = Y_{i-1,\, j},$$

$$s_2 Y_{i,j} = Y_{i,\, j+1} \tag{4.1.2}$$

Then, the difference equations in (4.1.1) take the form,

$$Y_{ij} + \sum_{k=1}^{m} \theta_k s_1^{-q_k^1} s_2^{-q_k^2} Y_{ij} = \beta^{\frac{1}{2}} U_{ij} \quad 1 \leq i \leq N_1,\ 1 \leq j \leq N_2 \tag{4.1.3}$$

or more compactly,

$$\Theta(s_1, s_2) Y_{ij} = \beta^{\frac{1}{2}} U_{ij}, \tag{4.1.4}$$

where

$$\Theta(s_1, s_2) = 1 + \sum_{k=1}^{m} \theta_k \, s_1^{-q_k^1} \, s_2^{-q_k^2}. \tag{4.1.5}$$

Each such model is parametrized by the tuple, $(Q, \theta, N_1, N_2, \beta)$. We are now ready to state our algorithms.

Modeling Algorithm: (Known G_{ij} and B_{ij}).

Step 1: Choose a window/segment of size $N_1 \times N_2$ and construct a bathymetry model

$$(1 + \sum_{k=1}^{m_B} \theta_k^B \, s_1^{-q_k^1} s_2^{-q_k^2}) B_{ij} = \sqrt{\beta^B} \, U_{ij}^B \tag{4.1.6}$$

Step 2: Using the same window/segment construct a gravity model

$$(1 + \sum_{k=1}^{m_G} \theta_k^G \, s_1^{-q_k^1} s_2^{-q_k^2}) G_{ij} = \sqrt{\beta^G} \, U_{ij}^G \tag{4.1.7}$$

Step 3: Investigate whether the *residual field,*

$$W_{ij} = - \sqrt{\beta^B} \, U_{ij}^B + \sqrt{\beta^B} \, U_{ij}^G$$

passes a *whiteness test,* e.g. by explicitly estimating the correlation function of W_{ij}. If it does not then construct a *residual model* of the form,

$$(1 + \sum_{k=1}^{m_W} \theta_k^W \, s_1^{-q_k^1} \, s_2^{-q_k^2}) W_{ij} = \sqrt{\beta^W} \, U_{ij} \tag{4.1.8}$$

where U_{ij} is a standard white noise field.

Step 4: We now obtain a model relating gravity and bathymetry,

$$\begin{aligned} &(1 + \sum_{k=1}^{m_G} \theta_k^G s_1^{-q_k^1} s_2^{-q_k^2}) G_{ij} \\ &= (1 + \sum_{k=1}^{m_B} \theta_k^B \, s_1^{-q_k^1} s_2^{-q_k^2}) B_{ij} + \\ &+ (1 + \sum_{k=1}^{m_W} \theta_k^W \, s_1^{-q_k^1} \, s_2^{-q_k^2})^{-1} \sqrt{\beta^W} \, U_{ij} \, . \end{aligned} \tag{4.1.9}$$

Clearly, this can be written in the form,

$$\Theta^W(s_1,s_2)\cdot\Theta^G(s_1,s_2)G_{ij} = \Theta^W(s_1,s_2)\Theta^B(s_1,s_2)B_{ij} + \sqrt{\beta^W}U_{ij} \tag{4.1.10}$$

The model is parametrized by the following neighborhood sets Q^B, Q^G, Q^W, the weight vectors θ^B, θ^G, θ^W and the window size $N_1 \times N_2$.

We can write (4.1.10) compactly in the form,

$$M(s_1,s_2)\, G_{ij} = N(s_1,s_2)B_{ij} + \sqrt{\beta^W}U_{ij}, \tag{4.1.11}$$

where,

$$N(s_1,s_2) = \Theta^W(s_1,s_2).\ \Theta^B(s_1,s_2) = 1 + \sum_{k=1}^{m(\nu)} \nu_k s_1^{-q_k^1} s_2^{-q_k^2} \tag{4.1.12}$$

and

$$M(s_1,s_2) = \Theta^W(s_1,s_2)\Theta^G(s_1,s_2) = 1 + \sum_{k=1}^{m(\mu)} \mu_k s_1^{-q_k^1} s_2^{-q_k^2} \tag{4.1.13}$$

where $m(\mu)$ and $m(\nu)$ are positive integers determined by m^W, m^B and m^G.

Suppose we are now presented with gravity data from a region of the earth which is *geophysically similar* to the region from which the data for gravity and bathymetry used in constructing the model (4.1.11) was obtained. It is now required to infer the bathymetry for this new region. We simply *postulate* that the model (4.1.11) applies in the new region as well. In this new region, the inversion process has thus two steps.

Inversion from G_{ij} *to* B_{ij} :

Step 1: Postulate a model of the form,

$$M(s_1,s_2)G_{ij} = N(s_1,s_2)B_{ij} + \sqrt{\beta^W}U_{ij}$$

with known polynomials M and N and coefficient β^W.

Step 2: Given gravity data G_{ij} in the new region solve for B_{ij}, (e.g. by applying least squares to the above model or by constrained least squares if some partial bathymetry constraints are at hand).

From the discussion above, it should be apparent that the key modeling process involves constructing three periodic random field models associated to the poynomials, $\Theta^G(s_1,s_2)$, $\Theta^B(s_1s_2)$ and $\Theta^W(s_1,s_2)$, all of the same generic form (4.1.1)-(4.1.2). In the next section we explain the basic steps in this estimation problem.

4.2. Estimation of a Generic Univariate Autoregressive Periodic Random Field:

In this section we will continue to use the notation of section (2.3). First we recall the notion of a circulant matrix, i.e. a matrix of the form

$$\text{circulant}\,(\lambda_1,\ldots,\lambda_n) \triangleq \begin{bmatrix} \lambda_1 & \lambda_2 & & & \lambda_n \\ \lambda_n & \lambda_1 & \lambda_3 & \cdots & \lambda_{n-1} \\ \lambda_{n-1} & \lambda_n & \lambda_2 & \cdots & \lambda_{n-2} \\ \cdot & \cdot & \lambda_1 & \cdots & \cdot \\ \cdot & \cdot & \lambda_4 & \cdots & \cdot \\ \lambda_2 & \lambda_3 & & & \lambda_1 \end{bmatrix} \qquad (4.2.1)$$

Now, given (2.3.1) together with the boundary condition (2.3.2), it is easy to see that the following holds:

$$\begin{bmatrix} A_1 & A_2, & A_3 & \cdots & A_{N_1} \\ A_{N_1} & A_1, & A_2 & \cdots & A_{N_1-1} \\ \cdot & \cdot & \cdot & \cdots & \cdot \\ \cdot & \cdot & \cdot & \cdots & \cdot \\ \cdot & \cdot & \cdot & \cdots & \cdot \\ A_2 & A_3 & A_4 & \cdots & A_N A_1 \end{bmatrix} \begin{bmatrix} y_1 \\ y_2 \\ \cdot \\ \cdot \\ \cdot \\ y_{N_1} \end{bmatrix} = \sqrt{\beta} \begin{bmatrix} u_1 \\ u_2 \\ \cdot \\ \cdot \\ \cdot \\ u_{N_1} \end{bmatrix} \tag{4.2.2}$$

where,

$$y_i = (Y_{i,1}, Y_{i,2}, \ldots, Y_{i,N_2})^T$$

and $u_i = (U_{i,1}, U_{i,2}, \cdots, U_{i,N_2})^T$. The matrices $A_1, A_2, \ldots,$ are all $N_2 \times N_2$ circulant matrices depending on the parameter θ and on Q. For the example set Q of section (2.3)

$$\begin{aligned} A_i &= 0 \quad \forall i \neq 1,2,N_1, \\ A_1 &= \text{Circulant } (1,\theta_3,0,\ldots,0,\theta_1) \\ A_2 &= \text{Circulant } (\theta_4,\theta_5,0,\ldots 0) \\ A_{N_1} &= \text{Circulant } (\theta_2,0,0,\ldots 0). \end{aligned} \tag{4.2.3}$$

The linear equation system (4.2.2) has a block circulant matrix structure also, i.e.

$$B(\theta)y = \sqrt{\beta}u \tag{4.2.2'}$$

where,

$$B(\theta) = \text{block circulant } (A_1, A_2, \ldots, A_{N_1})$$

is an $N_1N_2 \times N_1N_2$ matrix.

We are seeking a *maximum likelihood* estimate for θ. For this we need to write an expression for the *likelihood function* for the field $\{Y_{ij}\}$ or equivalently the random vector y. Since the right hand side of (4.2.2') is an N_1N_2 length Gaussian vector, it follows that the likelihood function is,

$$L(\theta,\beta) = \frac{[Det(B(\theta))}{(\sqrt{2\beta\pi}^{N_1N_2}} \prod_{\substack{i,j \\ 1\le i\le N_1 \\ 1\le j\le N_2}}$$

$$\exp\{ - \frac{1}{2\beta}(Y_{ij} + \sum_{k=1}^{m} \theta_k Y_{i+q_k^1, j+q_k^2})^2\} \tag{4.2.4}$$

Kashyap [Kashyap 1980, Image Modeling] has shown that,

$$Det(B(\theta)) = \prod_{i=0}^{N_1-1} \prod_{j=0}^{N_2-1} | | A(z_1^i, z_2^i, \theta) | | \tag{4.2.5}$$

where,

$$A(z_1,z_2,\theta) \triangleq 1 + \sum_{k=1}^{m} \theta_k (z_2)^{q_k^1} (z_1)^{q_k^2} \tag{4.2.6}$$

and

$$z_i = exp[\frac{2\pi\sqrt{-1}}{N_i}] \quad i=1,2. \tag{4.2.7}$$

We can now carry out a maximum (log) likelihood estimation procedure for the unknown parameters (θ,β) using the finite data set $\{Y_{i,j}: 1\le i\le N, 1\le j\le N_2\}$. Note,

$$\ln(L(\theta,\beta)) = - \frac{(N_1N_2)}{2} \ln(2\pi\beta)$$

$$- \frac{1}{2\beta} \sum_{i=1}^{N_1} \sum_{j=1}^{N_2} [Y_{ij} + \sum_{k=1}^{m} \theta_k Y_{i+q_k^1, j+q_k^2}]^2 \tag{4.2.8}$$

$$+ \frac{1}{2} \sum_{i=0}^{N_1-1} \sum_{j=0}^{N_2-1} \ln(| | A(z_1^i, z_2^j, \theta) | | ^2)$$

Maximizing $\ln(L(\theta,\beta))$ with respect to θ and β yields the estimates,

$$\theta^* = arg[\min \tilde{L}(\theta)]$$

$$\beta^* = \frac{1}{N_1N_2} \sum_{i=1}^{N_1} \sum_{j=1}^{N_2} [Y_{ij} + \sum_{k=1}^{m} \theta_k^* Y_{i+q_k^1, j+q_k^2}]^2 \tag{4.2.9}$$

where,

$$\tilde{L}(\theta) = N_1 N_2 \ln[\sum_{i=1}^{N_1}\sum_{j=1}^{N_2}(Y_{ij} + \sum_{k=1}^{m}\theta_k Y_{i+q_k^1, j+q_k^2})^2]$$

$$- \sum_{i=0}^{N_1-1}\sum_{j=0}^{N_2-1}\ln(|\,|A(z_1^i, z_2^j, \theta)|\,|^2) \tag{4.2.10}$$

The first term in $L(\theta)$ has a minimum at,

$$\bar{\theta} = [\sum_{i=1}^{N_1}\sum_{j=1}^{N_2} Y_{ij}^{Q})^T]^{-1} \sum_{i=1}^{N_1}\sum_{j=1}^{N_2} Y_{ij}^{Q} Y_{ij} \tag{4.2.11}$$

where,

$$Y_{ij}^{Q} \triangleq (Y_{i+q_1^1, j+q_1^2}, \ldots, Y_{i+q_m^1, j+q_m^2})^T \tag{4.2.12}$$

The formula (4.2.11) is very useful since it provides a quick estimate which is quite close to the *optimal* θ^*. In fact, one may use a Newton-Raphson technique to iterate from $\bar{\theta}$ to θ^*.

Everything we have done so far has hinged on a particular choice of neighborhood of dependence Q. The appropriate choice of neighborhood may be decided upon by considering several different neighborhoods $Q_1, Q_2, \ldots, Q_R$ and corresponding to each Q_k, compute

$$C_k \triangleq N_1 N_2 \ln \beta_k^* - \sum_{i=0}^{N_1-1}\sum_{j=0}^{N_2-1} \ln |\,|A_k(z_1^i, z_2^j, \theta_k^*)|\,|^2 \tag{4.2.13}$$

where β_k^*, θ_k^* are maximum likelihood estimates of the β_k, θ_k in the model corresponding to Q_k. The decision rule for determining the neighborhood of choice is

select that Q_k which minimizes C_k, for $k \in \{1,2,\ldots,R\}$.

See [Chellappa Kashyap Ahuja 1979 Decision rules neighbors] for details.

4.3. Segmentation/Window Determination:

Our main goal is to describe a method that will assist us in identifying the window size $N_1 \times N_2$ over which one can expect to be able to build a satisfactory homogeneous model for the gravity and bathymetry fields. Our idea here is that if one can find in a given data set (gravity or bathymetry) the *edges* across which there are significant changes in field intensity, then the edges can be used as boundaries of segments/windows. The subject of segmentation/edge detection in image processing has a very large literature. See the book [Rosenfeld 1981 Image Modeling] for diverse points of view. Kashyap himself suggests a statistical technique based on hypothesis testing for his models. We find that his methods are rather computation-intensive and we present an alternative originally arising in the thesis of Canny [Canny 1983 Edges and Lines]. The method is well-motivated from a signal processing point-of-view unlike a number of ad-hoc procedures in the literature. For instance, it brings together considerations of signal-to-noise ratio and localization into the design of the edge-detector. It leads to algorithms with tunable parameters which can be selected to adjust detector performance. It is possible to motivate the main ideas by using a *one dimensional model.*

4.3.1. A One-Dimensional Edge Model:

Consider a one dimensional image/field of the form,

$$I(x) = Au(x) + n(x) \qquad (4.3.1.1)$$

where A is a constant, n(x) is noise and u(x) is the unit step:

$$u(x) = \begin{cases} 1 & x \geq 0 \\ 0 & x < 0 \end{cases} \tag{4.3.1.2}$$

Our goal is to construct a procedure for detecting the edge $u(\cdot)$ in the noisy image $I(\cdot)$ and to localize it. We consider the following scheme:

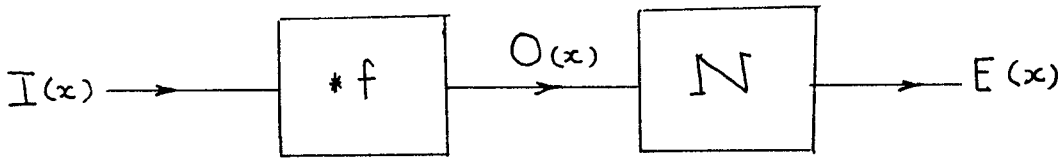

Figure 4.3.1

Here *f denotes convolution by a suitable kernel function f and N denotes the nonlinear operation of suppressing all but the local minimum in O(x). The output of N is supposed to be the edge/step. The first (linear) processor is chosen to be a convolution by *requiring translation invariance* (i.e. insensitivity to the location of the edge - here the point x=0).

Now,

$$O(0) = A \int_{-\infty}^{\infty} f(x)u(-x)dx \tag{4.3.1.3}$$

$$+ \int_{-\infty}^{\infty} f(x)n(-x)dx$$

$$= \overset{A}{\not{e}} \int_{-\infty}^{0} f(x)dx + \int_{-\infty}^{\infty} f(x)n(-x)dx \quad . \tag{4.3.1.4}$$

Assume that n(x) is spatial white noise with zero mean and "variance parameter" σ_n^2. Clearly, O(0) is a random variable with mean $= A \int_{-\infty}^{\infty} f(x)dx$ and the spec-

tral energy of O(0) (or O(x)) arising from the noise alone is given by,

$$E[\int_{-\infty}^{\infty} f^2(x)n^2(-x)dx] \tag{4.3.1.5}$$

The output signal-to-noise ratio SNR is given by

$$\text{S.N.R.} = \frac{A\int_{-\infty}^{0} f(x)dx}{\sigma_n\sqrt{\int_{-\infty}^{\infty} f^2(x)dx}} \tag{4.3.1.6}$$

It is desirable to choose 'f' in order to make, SNR as large as possible.

4.3.2 . The Localization Problem:

Since the nonmaximum suppression operation marks zero crossings of $\frac{d}{dx}O(x)$ as edge points, and since,

$$\begin{aligned} O &= O'(x) \\ &= O_s'(x) + O_n'(x) \\ &= A\,f(x) + \int_{-\infty}^{\infty} f'(y)n(x-y)dy, \end{aligned} \tag{4.3.2.1}$$

it can be shown that, under the assumption that f(x) = -f(-x), the quantity,

$$L = \frac{A\,|f'(0)|}{\sigma_n\sqrt{\int_{-\infty}^{\infty} f'^2(x)dx}} \tag{4.3.2.2}$$

is a measure of the degree of localization. If L is large then the standard deviation of the distance of the actual maximum to the true edge is small. Consider,

$$\Sigma = \Sigma(f) = \frac{\int_{-\infty}^{0} f(x)dx}{\sqrt{\int_{-\infty}^{\infty} f^2(x)dx}} \tag{4.3.2.3}$$

$$\Lambda = \Lambda(f) = \frac{|f'(0)|}{\sqrt{\int_{-\infty}^{\infty} f'^{2}(x)dx}} \tag{4.3.2.4}$$

Both Σ and Λ are independent of the *magnitude scales* for f. Furthermore, suppose we do spatial scaling,

$$f(\cdot) \rightarrow f_w(\cdot)$$

where,

$$f_w(x) = f(x/w).$$

Then, it can be verified that,

$$\Sigma(f_w)\Lambda(f_w)$$

$$= \left[\frac{\sqrt{w}\int_{-\infty}^{0} f(x)dx}{\sqrt{\int_{-\infty}^{\infty} f^{2}(x)dx}}\right]\left[\frac{1}{\sqrt{w}}\frac{|f'(0)|}{\sqrt{\int_{-\infty}^{\infty} f'^{2}(x)dx}}\right] \tag{4.3.2.5}$$

$$= \Sigma(f)\Lambda(f)$$

Thus localization can be traded off against detection performance. A 'broad' function $f(\cdot)$ will have good signal to noise ratio but poor localization compared to a filter with a narrow $f(\cdot)$. One could now try to find $f(\cdot)$ that maximizes $\Sigma(f)\Lambda(f)$. One can also, for computational ease, try to find f that maximizes $\Lambda(f)$ while $\Sigma(f) = c_1$ is fixed *or* find f that maximizes $\Sigma(f)$ while $\Lambda(f) = c_2$ is fixed. The corresponding Euler- Lagrange equations yield explicit families of $f(\cdot)$ that are appropriate as filters [Canny 1983 Edges Lines].

The principal defect of the above approach is that it does not take into account the possibility multiple edge responses from the detector caused by noise. From the basic edge detection scheme (see figure 4.3.1), it is clear that such multiple detector responses are due to zero crossings in the derivative of the output of the linear filter. These (random) zero crossings can be estimated by a formula due to S. Rice and we are lead to an optimization problem of the form,

$$\text{minimize} \int_{-W}^{0} (f^2 + \lambda_1 f'^2 + \lambda_2 f''^2 + \lambda_3 f)\,dx \qquad (4.3.2.6)$$

where λ_1, λ_2, λ_3, are Lagrange Multipliers.

Analysis of the corresponding Euler-Lagrange equations leads to a family of solutions,

$$f(x) = a_1 e^{-ax} \sin(\omega x) + a_2 e^{ax} \cos(\omega x)$$

$$+ a_3 e^{-ax} \sin(\omega x)$$

$$+ a_4 e^{-ax} \cos(\omega x) + c$$

with boundary conditions,

$$f(0) = 0 = f(-W)$$

$$f'(0) = s\,;\ f'(-W) = 0.$$

These lead to conditions on the parameters a_i and c, in terms of s. We omit the details.

The nonlinear processor N for nonmaximum suppression is quite standard in the literature on edge detection/segmentation and we refer to page 81 of [Canny 1983 Edges and Lines].

We have implemented a discrete 2-D version of the above edge detection algorithm involving the following steps.

Let $I(i,j)$ be the given image. Let $\{h(j)\}$ the discrete convolutor.

Step 1: Compute Y(1,J),

$$Y_1(i,j) = \sum_{l=1-\infty}^{\infty} h(j-l)I(i,l)$$

Step 2: Compute X(1,J)

$$X(i,j) = \sum_{l=-\infty}^{\infty} h(i-l)Y(l,j)$$

Step 3: Do nonmaximum suppression. The above infinite convolutions are truncated; since we use,

$$h_k = e^{-\lambda k} \cos(\omega k) \quad k = 0,1,2,\ldots$$

$$h_{-k} = -h_k \qquad k = 0,1,2,\ldots$$

it is possible to implement the above algorithm using *fast convolutions.* The parameter,

$$\lambda = \frac{1}{\sigma} > 0,$$

and

$$\omega = 0.8\lambda.$$

Tuning σ gives us control of performance. A smaller value of σ give us good localization, while a bigger value of σ picks up global features. A series of computer experiments were performed on a VAX 11/780 computer at the Computer Vision Laboratory at the University of Maryland, using digitized pictures of real scenes and objects. By tuning the σ parameter appropriately it was possible to

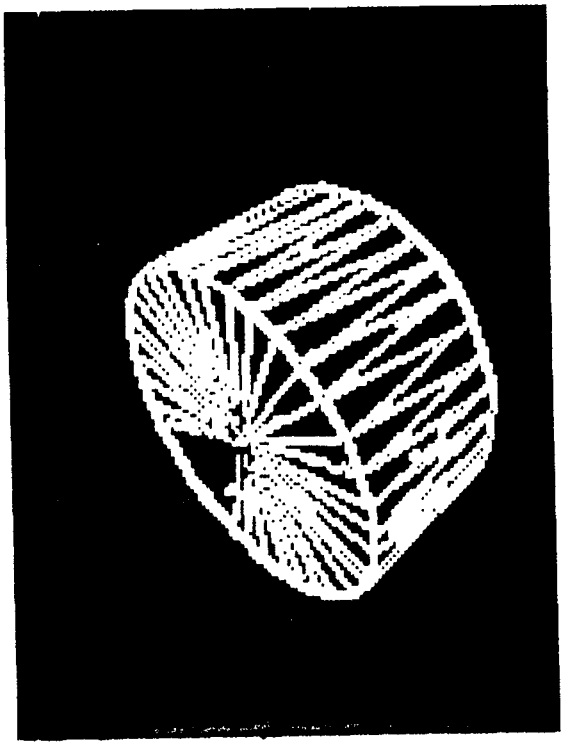

(b)

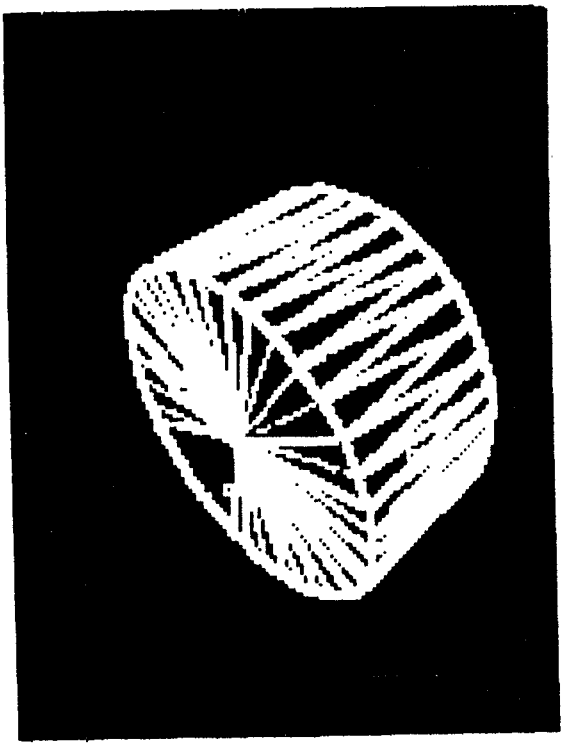

(c)

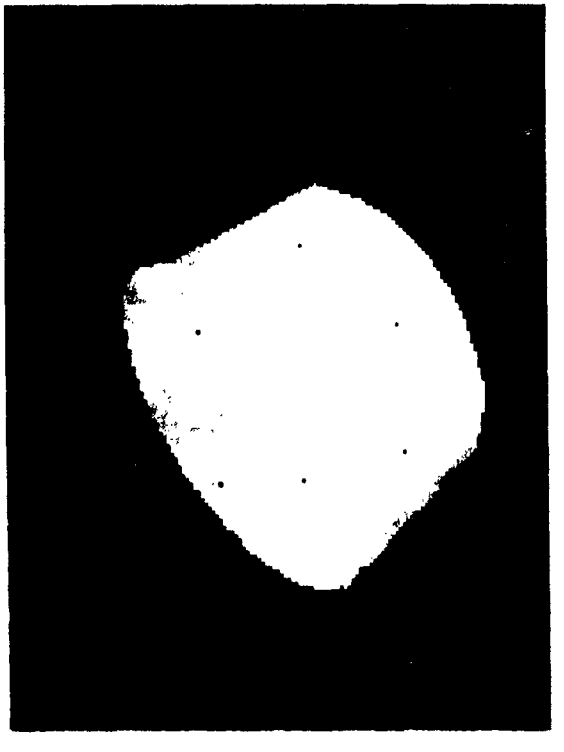

(a)

Figure 4.4.1

(a) object

(b) Canny detector
$\lambda = 3.45$
$\omega = 0.7$

(c) Sobel mask

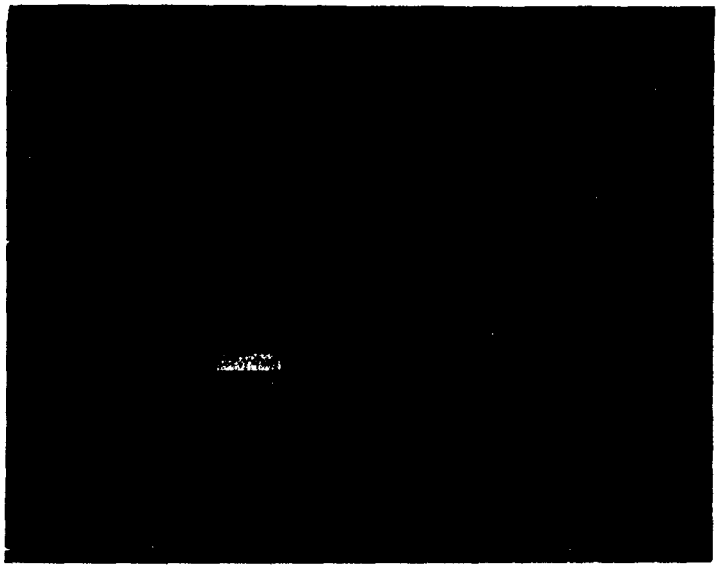

(d)

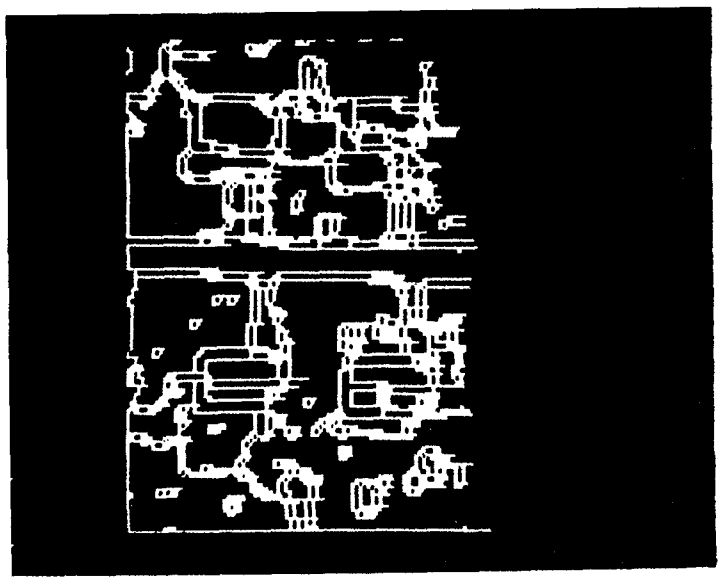

(e)

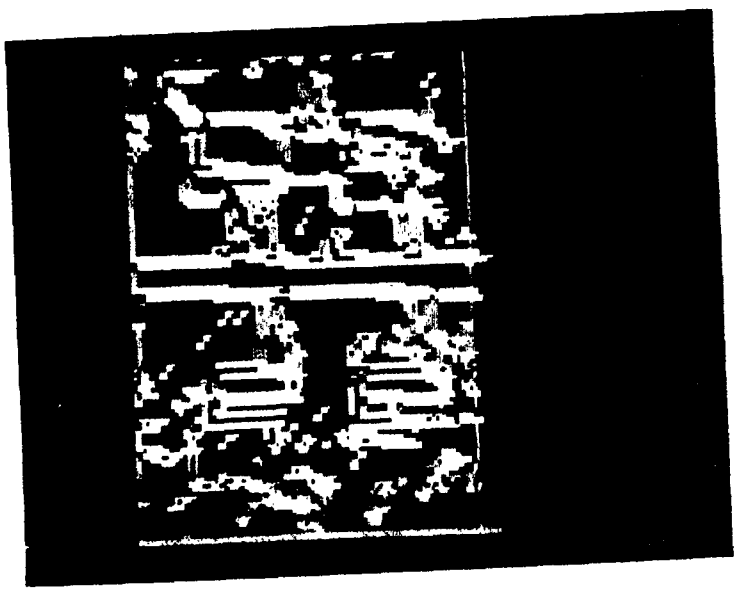

(f)

Figure 4.4.1

(d) urban scene

(e) Canny detector, parameters same as in figure 4.4.1 (b)

(f) Sobel mask

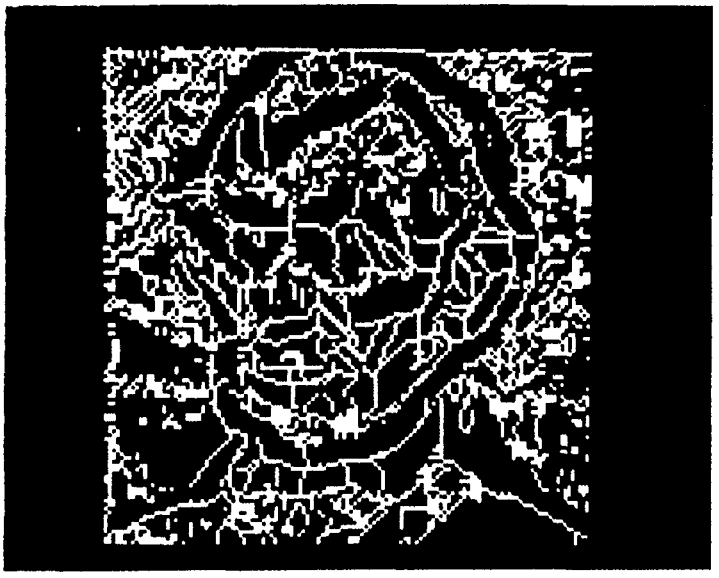

(h)

(g)

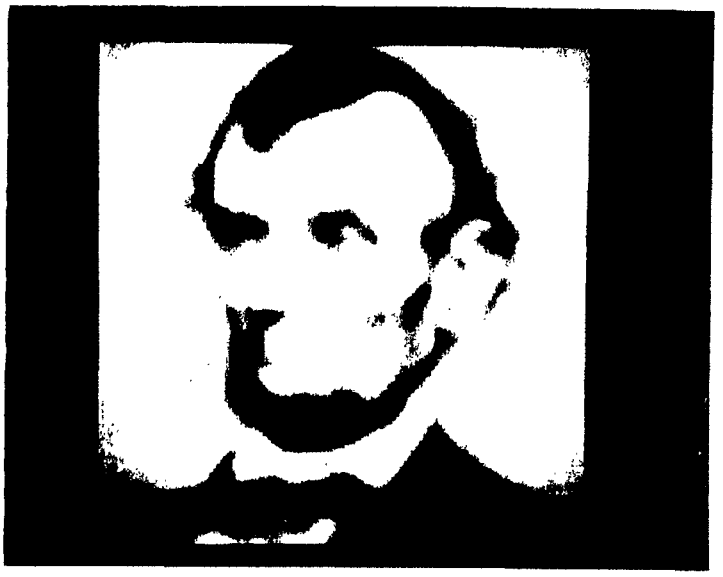

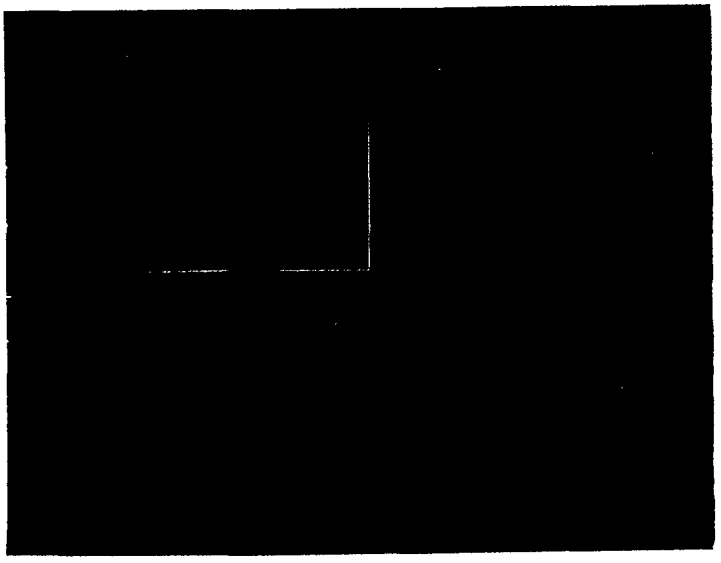

Figure 4.4.1

(g) portrait

(h) Canny detector

λ = +1.0

ω = 0.7

Note: all pictures with 255 gray levels, image sizes 128 x 128 pixels.

often obtain better performance in edge detection than with the help of a traditional algorithm such as the one based on a differencing mask due to Sobel. Some typical pictures are included (see Figure 4.4.1).

4.4. Some Recent Advances in Deconvolution:

Here we note rather briefly how some new developments in deconvolution may be useful for geophysical inversion.

Many observation models in geophysical exploration take the form,

$$f * \mu_i \triangleq \int_{\mathbb{R}^2} f(x-y)\,d\mu_i(y) = g_i(x) \quad i=1,2,\ldots,N \quad . \tag{4.4.1}$$

where μ_i is a distribution of compact support over a region in $\mathbb{R}^{n^2}$ defining an observation process and $f(\cdot)$ denotes an unknown geophysical field to be determined (e.g. density anomaly) and $g_i(\cdot)$ denotes the corresponding observation (gravity anomaly, magnetic anomaly etc.). The indexing of the observation data set by $i \in \{1,2,\ldots,N\}$ may be used also to refer to multiple passes/tracks.

The inverse problem of interest to us is to determine $f(\cdot)$ given $g_i(\cdot)$, $i \in \{1,2,\ldots,N\}$. We call this a *deconvolution problem involving multisensors.* If however, only one data set say g_1 is available, then it is well-known that the inverse proble is ill-posed -- the inverse opertor is typically unbounded -- and leads to serious issues of numerical accuracy. Various regularization techniques are known for the problem of approximate reconstruction of $f(\cdot)$.

On the other hand, if we have multiple sensors, and if we can solve for ν_i in the equation,

$$\nu_1 * \underset{1}{\mu} + \nu_2 * \underset{2}{\mu} + \cdots + \nu_N * \underset{N}{\mu} = \delta \tag{4.4.2}$$

where δ denotes the Dirac delta function, then it is clear that we have a reconstruction formula,

$$f = \nu_1 * g_1 + \nu_2 * g_2 + \cdots + \nu_N * g_N \ . \tag{4.4.3}$$

By taking Fourier transforms of both sides in (4.4.2), we obtain the equivalent form,

$$\hat{\nu}_1\hat{\mu}_1 + \hat{\nu}_2\hat{\mu}_2 + \cdots + \hat{\nu}_N\hat{\mu}_N = 1 \ . \tag{4.4.4}$$

Equation (4.4.4) is known as the *Bezout equation.* In their fundamental work, Berenstein, Taylor and Yger obtained explicit formulas for the deconvolutors $\nu_1,\ldots,\nu_N$, for certain classes of problems. The key requirement here is that, in order for the existence of the deconvolutors $\nu_1, \ldots, \nu_N$ (equivalently, solvability of the Bezout equation), the functions $\hat{\mu}_1,\ldots\hat{\mu}_N$ should satisfy a coprimeness condition, i.e., in a strong sense, these Fourier transforms *should not have common zeros.*

In a long report [Berenstein Krishnaprasad Taylor 1985 Deconvolution methods], the authors undertook a detailed numerical study of a special class of examples. These examples involved two sensors (N=2) and the observation map corresponded to averaging over an interval a_i, $i=1,2,$; thus

$$g_i(x) = \frac{1}{2a_i} \int_{x-a_i}^{x+a_i} f(y)dy \qquad i=1,2 \ . \tag{4.4.5}$$

the corresponding Fourier transforms $\hat{\mu}_1$ and $\hat{\mu}_2$ are given by

$$\hat{\mu}_i = \frac{\sin(a_i x)}{a_i x} \qquad i=1,2 \ . \tag{4.4.6}$$

The necessary and sufficient condition for strong coprimeness (solvability of the Bezout equation) turns out to be:

$$a_1/a_2 \quad \text{is irrational !!} \tag{4.4.7}$$

In the paper [Berenstein Krishnaprasad Taylor 1985] extensive numerical studies were conducted, using $a_1=1$, $a_2=\sqrt{2}$. The techniques applied to the problem of resolving peaks in a double Gaussian proved to be remarkably robust.

Our main point here is that it would be very useful to try and attempt a study of the suitability of the above deconvolution methods to problems of geophysical inversion. As a first step we suggest the use of this method on transfer function models relating bathymetry and free air gravity.

5. Future Work:

In this section we make some preliminary recommendations for further development of our efforts in order to provide practical tools for basic geophysical modeling and inversion techniques. The pervasive theme of this report is that while many successful algorithms have been produced for these problems, these tend to be primarily based on 1-D processing. With the recent advances in the subject of discrete random fields, it is desirable to take advantage of new 2-D signal processing methods. There are several possible directions. As a first step, it is desirable to test the proposed 2-D statistical modeling and inversion techniques on synthetic and real data. Detailed sea-bottom models should be investigated with reference to their correlation properties.

5.1. Testing of Proposed Inversion Technique:

We suggest that the modeling and inversion techniques of section 4 be implemented and first tested on synthetic data of reasonable verisimilitude. Special attention should be given to the types of parameter ranges and Q neighborhoods involved. The segmentation algorithm should also be implemented and tested alongside.

It would be very natural to treat the 2-vector $(G_{ij}, B_{ij})^T$ as a bivariate random field and then proceed to construct models for it directly using data from regions where we know both gravity and bathymetry. However, at present this does not appear to be computationally feasible. It is for this reason that we have chosen to work with univariate field models. However, it is desirable that such bivariate modeling methods be further developed and fast algorithms should be investigated.

An important part of our methodology involves the modeling of bathymetry. It is desirable that detailed statistical studies of sea-bottom roughness be conducted in order to get some insight into this basic element of our methodology.

6. Acknowledgements:

As outsiders venturing for the first time into the rich subject of geophysical modeling, we have had to go through a rather long educational process. Conversations in this connection with L.C. Kovacs, M. Czarnecki and J. Brozena have been most helpful.

REFERENCES

1. N.K. Bose (1982), *Multidimensional System Theory,* Van Nostrand Reinhold, New York.

2. G.E.P. Box and G.M. Jenkins (1971), *Time Series Analysis in Forecasting and Control,* Holden-Day, New York.

3. M.S. Bartlett (1976), *The Statistical Analysis of Spatial Pattern,* Chapman and Hall, London.

4. E.J. Hannan (1960), *Time Series Analysis,* Methuen, London.

5. R.L. Kashyap (1981), Univariate and multivariate random field models for images, pp. 245-258, in ed. A. Rosenfeld: *Image Modeling,* Academic Press, New York 1981.

6. R. Chellappa, R.L. Kashyap and N. Ahuja (1979), Decision rules for choice of appropriate neighbors, *Technical Report 802, Computer Science,* Univ. of Maryland, College Park.

7. R. Chellappa (1980), Spatial Autoregressions in digital image restoration: simultaneous models, *Technical Report TR-984, Computer Vision Laboratory,* Univ. of Maryland, College Park, (also AFOSR TR-81-0059), 23 pages.

8. D.W. Oldenburg (1974), The inversion and interpretation of gravity anomalies, *Geophysics,* Vol. 39, pp. 526-536.

9. B.K. Bhattacharyya and L.K. Leu (1975), Spectral analysis of gravity and magnetic anomalies due to two-dimensional structures, *Geophysics,* Vol. 40,

pp. 993-1013.

10. L.B. Pedersen (1978), A statistical analysis of potential fields using a vertical cylinder and a dike, *Geophysics,* Vol. 43, pp. 943-953.

11. L.B. Pedersen (1979), Wavenumber domain methods for fast interpretation of potential field data, *Geoexploration,* Vol. 17, pp. 205-221.

12. N.J. Fisher and L.E. Howard (1980), Gravity interpretation with the aid of quadratic programming, *Geophysics,* Vol. 45, No. 3, pp. 403-419.

13. B.J. Last and K. Kubik (1983), Compact gravity inversion, *Geophysics,* Vol. 48, No. 6, pp. 713-721.

14. G.D. Garland (1965), *The Earth's Shape and Gravity,* Pergamon Press, Oxford.

15. L.J. Rosenblum (1983), The gravity to bathymetry inversion algorithm, *Internal Memorandum,* Naval Research Laboratory, Washington, D.C.

16. A. Rosenfeld, ed. (1981), *Image Modeling,* Academic Press, New York.

17. J.F. Canny (1983), *Finding Edges and Lines in Images,* M.S. Thesis, Massachusetts Institute of Technology, (also *Technical Report No. 720,* MIT Artificial Intelligence Laboratory), Cambridge.

18. C.A. Berenstein, P.S. Krishnaprasad and B.A. Taylor (1985), *Deconvolution Methods for Multisensors.* (*Technical Report, MD 85-23-CB,* TR85-19, *Department of Mathematics,* Univ. of Maryland, College Park, 63 pages (Also available as DTIC Report).